

Cepheid and Tip of the Red Giant Branch Distances To the
Dwarf Irregular Galaxy IC 10¹

SHOKO SAKAI

Kitt Peak National Observatory
P.O. Box 26732, Tucson, AZ 85726 shoko@noao.edu

BARRY F. MADORE

NED, California Institute of Technology
MS 100–22, Pasadena, CA 91125 barry@ipac.caltech.edu

WENDY L. FREEDMAN

The Observatories, Carnegie Institution of Astronomy
813 Santa Barbara St. Pasadena, CA 91101 wendy@ociw.edu

Running Headline: *TRGB Distance to IC 10*

Accepted for Publication in *Astrophysical Journal*

¹Based on observations made at Palomar Observatory as part of a continuing collaborative agreement between the California Institute of Technology and the Jet Propulsion Laboratory.

ABSTRACT

We present color-magnitude diagrams and luminosity functions of stars in the nearby galaxy IC 10, based on VI CCD photometry acquired with the COSMIC prime-focus camera on the Palomar 5m telescope. The apparent I-band luminosity function of stars in the halo of IC 10 shows an identifiable rise at $I \approx 21.7$ mag. This is interpreted as being the tip of the red giant branch (TRGB) at $M_V \approx -4$ mag. Since IC 10 is at a very low Galactic latitude, its foreground extinction is expected to be high and the uncertainty associated with that correction is the largest contributor to the error associated with its distance determination. Multi-wavelength observations of Cepheid variable stars in IC 10 give a Population I distance modulus of 24.1 ± 0.2 mag, which corresponds to a linear distance of 660 ± 66 kpc for a total line-of-sight reddening of $E(B-V) = 1.16 \pm 0.08$ mag, derived self-consistently from the Cepheid data alone. Applying this Population I reddening to the Population II halo stars gives a TRGB distance modulus of 23.5 ± 0.2 mag, corresponding to 500 ± 50 kpc. We consider this to be a lower limit on the TRGB distance. Reconciling the Cepheid and TRGB distances would require that the reddening to the halo is $\Delta E(B-V) = 0.31$ mag lower than that into the main body of the galaxy. This then suggests that the Galactic extinction in the direction of IC 10 is $E(B - V) \simeq 0.85$.

Subject headings: galaxies: individual (IC 10) – galaxies: dwarf galaxies – galaxies: distances

1. Introduction

IC 10 is a dwarf galaxy located at $\alpha = 00^h20^m.4$ and $\delta = 59^d18^m$ (2000). As the nearest example of a post–burst dwarf galaxy, IC 10 has been recognized as an important object particularly in studies of the interstellar medium and star formation in dwarf irregular galaxies. This galaxy has a heliocentric velocity of -344 ± 3 km s $^{-1}$ (RC3, 1991). However, the distance to IC 10 has been very poorly determined until recently. For almost three decades, the distance estimates for IC 10 have ranged between 1 and 3 Mpc. This uncertainty is largely attributable to the fact that IC 10 is located at a very low Galactic latitude, $b = -3^\circ$, and large extinction corrections need to be applied. One of the earliest distance estimates was reported by de Vaucouleurs & Ables (1965); their value of 1.25 Mpc was based on the largest “ring–like” HII regions. Judging from the large HI extent of the galaxy, Roberts (1962) also placed this galaxy at 1 Mpc. There were, however, subsequent studies that suggested a significantly larger distance for IC 10. For example, Sandage & Tammann (1974) reported that its distance was 3 Mpc, based on the size of the three largest HII regions. Using the HII rings again, de Vaucouleurs (1978) then suggested that IC 10 was at 2 Mpc; while an upper limit of 2.2 Mpc was suggested by Jacoby & Lesser (1981) from the observations of a single planetary nebula. Yahil et al. (1977) concluded that based on this galaxy’s degree of resolution into stars, it should be located at around 1.5 Mpc. Bottinelli et al. (1984) used a Tully–Fisher relation to determine the distance of 2 Mpc. However, unfortunately this was based on B–band photometry which required a large extinction correction.

Recent observations now suggest that IC 10 is a member of the Local Group. Studies of Wolf-Rayet stars by Massey & Armandroff (1995) first indicated that IC10 lies at a distance of only 950 kpc. Subsequently, Saha et al. (1996) discovered Cepheid variable stars, determining a distance of 830 kpc to IC 10. Infrared observations of these same Cepheids by Wilson et al. (1996) reported the distance of 820 kpc. Unfortunately, the color–magnitude diagram of Saha et al. (1996) did not penetrate deep enough to probe the red giant branch stars, even though they did in fact visually detect the background “Baade’s sheet” of red stars. These red giant branch stars can provide an independent, Population II measure of the distance to IC 10; and that is the subject of this paper. We also present the V and I Cepheid data from our frames and the distance using their period–luminosity relation. Furthermore, we derive the reddening correction estimate from the multi–wavelength observations of the Cepheid variables, compiled from new and previously published data.

As part of a continuing effort to obtain consistent distances to all the Local Group galaxies, we present in this paper, the detection and measurement of the tip of the red giant

branch (TRGB) in IC 10. The TRGB marks the helium core flash, which is detected in the I -band luminosity function as an abrupt discontinuity. The TRGB has been demonstrated observationally and shown theoretically to be an excellent distance indicator that is as accurate as the period–luminosity relation of Cepheid variable stars (Frogel, Cohen & Persson 1983, DaCosta & Armandroff 1990, Lee, Freedman & Madore 1993, Madore, Freedman & Sakai 1997 and references therein). The major advantage of the TRGB method over Cepheid variables is that its application is much quicker. In principle, only one epoch of observations is needed. The method can also be applied to any morphological type of galaxies. However, the limitation is that an independent estimate of reddening is required. This could pose additional uncertainties, especially in this particular application of IC 10, in which the errors in the reddening correction dominate the error in its distance estimate due to its low Galactic–latitude location.

2. Observations

Observations of IC 10 were made at Palomar Observatory using the Hale 5m telescope on two consecutive nights, October 5th and 6th, 1996. All the observations were done under photometric conditions, with moderate seeing (~ 1.2 arcsec). The Carnegie Observatories Spectroscopic Multislit and Imaging Camera (COSMIC, Kells et al. 1998), a prime focus camera, was used to obtain V and I -band images, with total exposure times being 480 and 600 sec for the first night, and 720 and 1080 sec for the second night. The data were debiased and flatfielded using standard reduction methods. Stellar photometry was obtained using the point–spread function fitting packages DAOPHOT and ALLSTAR (Stetson 1987), which use automatic star finding algorithms. A point spread function, as determined from bright, isolated stars in the same field, was then fit to extract total magnitudes.

A set of V and I standard stars, selected from Landolt’s catalog (1992), were observed at least once every hour throughout both nights, and the two nights were calibrated independently. The photometry comparison indicates that the zero–point calibrations of two nights are in excellent agreement; for both V and I , the magnitudes of brightest stars agree to within 0.01 mag. In the following sections, however, we will only present the data from the second night of observations, mainly because the telescope had moved slightly during the exposures of the first night. Thus, rather than combining the data from two nights, our analysis will focus on the second-night data only.

3. Luminosity Function and Color Magnitude Diagram

Figure 1 shows the COSMIC I -band image of IC10. We refer to the main body region within the inner ellipse as Region 1. The annular region between inner and outer ellipses is called Region 2, while the remainder of the frame is referred to as Region 3. In Figures 2a-c, a $(V - I)$ vs. I color-magnitude diagrams (CMD) of three regions in IC10 are shown.

In the main body, as observed from the CMD in Figure 2a, a red giant branch is present, as well as a sparse and ill-defined blue main sequence stellar population around $V - I \simeq 1.0$ mag extending from $I = 20.5$ down to 22.5 mag. Also present are some intermediate-age asymptotic giant branch (AGB) stars in the region slightly brighter than the RGB. The red giant branch is more clearly demonstrated in Figure 2b, for the halo region of IC 10. However, AGB stars are also present in this CMD and care must be exercised to discriminate between the position of the TRGB and AGB in the luminosity function (below). In Regions 2 & 3, the blue main sequence stars are no longer present, especially in Region 3; however, the foreground stars start dominating the CMD region at $V - I \simeq 1 - 3$ mag at brighter magnitudes between $I = 17$ and 20.5 mag.

Histograms in Figure 3 show the I -band luminosity functions for the stellar populations found in Region 1 (left) and Regions 2 & 3 of IC 10. In the Region 1 luminosity function, we see no distinct discontinuity at any point. In contrast, the main characteristic of the halo I -band luminosity function (Regions 2 and 3) is the jump by nearly 50% in counts (between adjacent bins 0.1 mag in width), at $I \simeq 21.7$ mag. This, we believe, marks the tip of the red giant branch, which is the focus of Section 5. There is also a jump, though significantly smaller than the one at 21.7 mag, at $I \sim 21.4$ mag. We ascribe this feature to the AGB population intrinsic to IC 10.

In the next section, we discuss the distance to IC 10 derived from Cepheid variable stars, which is then compared with the tip of the red giant branch method in the subsequent section.

4. Cepheid Variable Stars in IC 10

Saha et al. (1996) discovered 13 variable star candidates in IC 10, nine of which were identified as Cepheids or Cepheid-like stars. However, their observations were undertaken using Gunn *gri* filters. Here, we have recovered some of these Cepheids on our COSMIC frames and their V and I magnitudes are presented in Table 1. Unfortunately, the brighter Cepheid variables were saturated on our images, so we were unable to photometer some of the candidates. The V and I Cepheid data are plotted in Figure 4. They represent

random-phase period-luminosity (PL) relations; no phase corrections or averaging were applied.

The absolute calibrations for the PL relations are adopted from Madore & Freedman (1991) which are based on a consistent set of 25 Large Magellanic Cloud (LMC) Cepheid variables with $BVRGIJHK$ observations and expressed as:

$$M_V = -2.88(\pm 0.20)(\log P - 1.00) - 4.11(\pm 0.09)[\pm 0.29], \quad (1)$$

$$M_I = -3.14(\pm 0.17)(\log P - 1.00) - 4.84(\pm 0.06)[\pm 0.21]. \quad (2)$$

These calibrations assume values of $(m - M)_0 = 18.50 \pm 0.10$ mag and $E(B - V) = 0.10$ mag for the distance modulus and reddening of the LMC. The apparent distance modulus for the IC 10 data at each wavelength was determined by minimizing the rms deviations of the observed data about the ridge line, with the slopes fixed to those given by the above equations. For V and I , we obtain distance moduli, respectively, of $(m - M)_v = 27.87 \pm 0.11$ and $(m - M)_i = 25.98 \pm 0.14$; the shortest-period Cepheid (V6) with $P = 8$ d was omitted from these calculations, given its anomalous color and also as to avoid the possible influence of overtone pulsators.

Near-infrared magnitudes of four Cepheid variables in IC 10 are listed in Table 2 of Wilson et al. (1996). We follow the same procedures as above to obtain apparent distance moduli in JHK , using the following absolute calibration, again provided by Madore & Freedman (1991) based on 25 LMC Cepheids:

$$M_J = -3.31(\pm 0.11)(\log P - 1.00) - 5.29(\pm 0.05)[\pm 0.16], \quad (3)$$

$$M_H = -3.37(\pm 0.10)(\log P - 1.00) - 5.65(\pm 0.04)[\pm 0.14], \quad (4)$$

$$M_K = -3.42(\pm 0.09)(\log P - 1.00) - 5.70(\pm 0.04)[\pm 0.13]. \quad (5)$$

The J , H and K apparent distance moduli are $(m - M)_J = 25.62 \pm 0.23$, $(m - M)_H = 25.05 \pm 0.29$ and $(m - M)_K = 24.39 \pm 0.34$ respectively.

Following the procedure outlined in detail by Madore & Freedman (1991), a reddening law, consistent with Cardelli, Clayton & Mathis (1989), was fitted to the $VIJHK$

multi-wavelength apparent distance moduli, as shown in Figure 5. Extrapolating to $\lambda^{-1} = 0$, we obtain a true distance modulus of 24.10 ± 0.19 mag (660 ± 63 kpc), with a reddening of $E(B - V) = 1.16 \pm 0.08$ mag. Since the determination of the true distance modulus requires finding the minimum χ^2 solution in the extinction/modulus plane, the errors in these two variables are dependent on each other. Thus the uncertainties in the distance modulus are illustrated in the enclosed box in Figure 5 as χ^2 contour ellipses, ranging from 1 to $3 - \sigma$.

5. Detection of the Tip of the Red Giant Branch

The TRGB marks the core helium flash of old, low-mass stars. These stars evolve up the red giant branch, but almost instantaneously change their physical characteristics upon ignition of helium, which in turn appears as a sudden discontinuity in the luminosity function. In the I -band ($\sim 8200\text{\AA}$), the tip is observed at $M_I \simeq -4$ mag, and this magnitude has been shown both observationally and theoretically to be extremely stable; it varies only by ~ 0.1 mag for ages 2 – 15 Gyr, and for metallicities between $-2.2 < [\text{Fe}/\text{H}] < -0.7$ dex, (the range spanned by the Galactic globular clusters). Here, we use the calibration determined by Lee et al. (1993) which is based on the observations of four Galactic globular clusters by Da Costa & Armandroff (1990).

The foreground extinction value for IC 10 has been a major obstacle when determining the distance to this galaxy accurately, as IC 10 is located at the very low Galactic latitude of only $b = -3.3$. The estimate given by de Vaucouleurs & Ables (1965) of $E(B - V) = 0.87$ mag was used as a standard value for many years. Other estimates ranged from $E(B - V) = 0.4$ mag (de Vaucouleurs 1978) up to 1.7 – 2.0 mag (Yang & Skillman 1993). More recent studies by Massey & Armandroff (1995) used the Wolf-Rayet stars and the location of the main sequence blue plume to determine the foreground extinction value, and concluded $E(B - V) = 0.75 - 0.80$ mag. In this paper, we derive a value of $E(B - V) = 1.16 \pm 0.08$ mag, which was obtained from the multi-wavelength Cepheid observations in the previous section. Using conversions of $A_V/E(V - I) = 2.45$ and $R_V = A_V/E(B - V) = 3.2$ (Dean, Warren & Cousins (1978), Cardelli et al. (1989) and Stanek (1996)), we obtain $A_V = 3.71 \pm 0.26$ and $A_I = 2.19 \pm 0.15$. The uncertainty in the reddening estimate is one of the largest sources of systematic errors in the IC 10 distance. We note, however, that the extinction for the red giant branch stars is likely to be smaller than $E(B - V) = 1.16$ mag. The Cepheid variables are usually found in and around the star-forming regions of the main body of the galaxy, which probably suffer from more reddening than the halo region where the RGB stars are observed. However, in the case of

IC10, the foreground reddening dominates that internal to the galaxy.

The top panels in Figure 6 show I -band luminosity functions of the stars in Region 1 (left) and Regions 2 and 3 which were shown in Figure 3, but smoothed by a variable Gaussian whose dispersion is the photometric error for each star detected. A Sobel edge-detection filter is applied to the smoothed luminosity functions following an equation: $E(m) = \Phi(I + \sigma_m) - \Phi(I - \sigma_m)$, where $\Phi(m)$ is the luminosity function at magnitude defined at m . For the details of the Sobel filter application, readers are referred to the Appendix of Sakai, Madore & Freedman (1996). The filtered function output are shown in the bottom panel of Figure 6. The position of the TRGB is indicated by the highest peak in the filter output. The data used in Figure 6 include all the stars found in specified regions. Here, however, we are interested in the red giant branch luminosity function. Using the $(V - I)$ color information, we select a subsample of stars with $2.5 \leq V - I \leq 3.0$, effectively excluding the bluer foreground stars which are merely noise in our TRGB application. The results are shown in Figure 7a where both the histograms and smoothed luminosity functions are used to illustrate the position of the tip. The position of the TRGB is indicated by both the significant jump in the number counts, and also by the prominent peak in the edge-detection filter output. To demonstrate the effectiveness of this scheme in which we selectively use only a subset of the RGB population, we show the luminosity function histograms and filter output for RGBs of redder and bluer regions in Figure 7b. For the bluest sample ($2.0 \leq V - I \leq 2.5$), although the TRGB can be still detected at $I \simeq 21.7$ in the filter output, the luminosity function histogram does not exhibit any significant corresponding discontinuity. For the redder sample of $3.0 \leq V - I \leq 3.5$, it is nearly impossible to visually identify the TRGB position in its luminosity function. Using the $2.5 \leq (V - I) \leq 3.0$ sample, we conclude that the TRGB is detected at $I = 21.70 \pm 0.15$ mag. The ‘full width half maximum’ of the output response peak profile is used to estimate an uncertainty of ± 0.15 mag on the apparent modulus.

5.1. TRGB Distance to IC 10

To calculate the true modulus to IC 10, we use the TRGB calibration of Lee et al. (1993), according to which the tip distance is determined via the relation $(m - M)_I = I_{TRGB} - M_{bol} + BC_I$, where both the bolometric magnitude (M_{bol}) and the bolometric correction (BC_I) are dependent on the color of the TRGB stars. They are defined by: $M_{bol} = -0.19[Fe/H] - 3.81$ and $BC_I = 0.881 - 0.243(V - I)_{TRGB}$. The metallicity is in turn expressed as a function of the $V - I$ color: $[Fe/H] = -12.65 + 12.6(V - I) - 3.3(V - I)^2$. The colors of the red giant stars, corrected for reddening, range from $(V - I)_0 = 0.6 - 1.6$

(see Figure 2), which gives the TRGB magnitude of $M_I = -4.00 \pm 0.10$. We thus derive the TRGB distance modulus of IC 10 to be $(m - M) = 23.51 \pm 0.19$ mag, *adopting the reddening of $E(B - V) = 1.16$, derived from the combined observations of the optical and IR Cepheid variable stars*. This corresponds to a linear distance of 500 ± 48 Kpc. The sources of errors include the uncertainties in (1) the tip position (0.05 mag), (2) reddening (0.15 mag) and (3) TRGB calibration (0.10 mag). This is the lower limit on the TRGB distance as the extinction in the halo is likely less than that in the main body of the galaxy where the Cepheid variables are detected.

The fact that the TRGB method requires an *independent* estimate of the reddening is a clear disadvantage, unlike the multi-wavelength Cepheid observations. This is especially problematic in the case of IC 10. In Table 2 we present various estimates of $E(B-V)$ for IC 10 and the corresponding values for A_V and A_I . Also tabulated are the true modulus and linear distance one would obtain using our TRGB magnitude combined with the suggested reddening. Distance estimates cover a factor of $4\times$, ranging from 230 up to 950 kpc, depending on the adopted reddening. The Cepheid-based distances derived by Saha et al. (1996: 830 ± 120 kpc) and Wilson et al. (1996: 820 ± 80 kpc) reduce to 660 ± 63 kpc when JHK data of Wilson et al. are combined with the VI data, reported here. This is directly a result of an increased reddening estimate derived from the multiwavelength data.

We consider the TRGB distance of 500 kpc that we obtain using the Cepheid reddening to be a lower limit, given that the line-of-sight reddening appropriate to the halo of IC 10 (where the red giant stars used in our analysis are located) is expected to be smaller than that of the main body of the galaxy where the Population I Cepheids, dust and gas are primarily concentrated. Without an independent measure of the reddening along the line-of-sight to the halo of IC 10, one alternative is to adopt the Cepheid distance, and then deduce the line-of-sight reddening to the halo. These two alternatives are illustrated by the color magnitude diagrams in Figure 8. On the left-hand side is the CMD in which the V and I magnitudes have been shifted by the TRGB distance derived using the extinction derived in this paper from the optical/IR Cepheid observations. Overplotted lines represent red giant branches of six Galactic globular clusters presented in Da Costa & Armandroff (1990); they do not quite match the IC 10 RGB. It is clear that the adopted distance modulus of 23.51 does not yield a consistent view. On the other hand, we can adopt the Population I Cepheid distance modulus of $m - M = 24.10$ as the true distance to IC 10. This would then mean the line-of-sight reddening to the halo of IC 10 becomes $E(B - V)_{\text{foreground}} \sim 0.85$ mag. The corresponding CMD is shown on the left-hand side of Figure 8. The IC 10 RGB matches well with those of the Galactic globular clusters, suggesting that the lower extinction in the halo region is a more sensible value to adopt here.

Even for the case presented on the right in Figure 8, we note that the Galactic globular cluster isochrones do not match the IC 10 RGB population very well. For example, there are a few stars observed at metallicities higher than the most metal-rich isochrone, and also in the bluer region. The metallicity of IC 10, measured from the observations of HII regions, is reported as $12 + \log(O/H) = 8.2$, which is similar to NGC 6822. Although this is a Pop I metallicity measurement, we do not expect the Pop II RGB metallicity to be much higher than this. The detection of stars “outside” the globular cluster isochrone range is likely due to a combination of several factors. First, the photometric errors for stars of fainter magnitudes at $I \geq 22.0$ reach $0.3 - 0.5$ mag. Thus, the stars with unreasonable colors could be simply due to uncertain photometric results. Second, the crowding probably plays a major role. When examining those stars in question more closely on the CCD images, a significant number of them in fact are located close to the foreground stars, star clusters, or HII regions. Variable reddening undoubtedly affects the photometric results as well. From our data alone, it is impossible to correct for such an effect, not to mention to estimate the degree of the reddening variation.

6. Summary

Using V and I photometry, the distance to a dwarf irregular galaxy, IC 10, has been determined using both the multi-wavelength Cepheid PL relation (Pop I) and the tip of the red giant branch method (Pop II). Adopting a total line-of-sight color excess of $E(B - V) = 1.16 \pm 0.19$ mag based on the Cepheid photometry, we derive the Population I distance of $(m - M) = 24.10 \pm 0.19$ (660 ± 63 kpc). Adopting this reddening yields the Population II distance of $(m - M) = 23.41 \pm 0.19$ (481 ± 45 kpc), which is a lower limit as the line-of-sight extinction in the halo region is smaller than that in the main body of the galaxy. If we adopt the Cepheid distance as the true distance to IC 10, it would then imply that the foreground reddening in the line-of-sight to the halo of IC 10 is $E(B - V)_{\text{foreground}} \sim 0.85$ mag.

This work was funded by NASA LTSA program, NAS7-1260, to SS. BFM was supported in part by the NASA/IPAC Extragalactic Database.

REFERENCES

- Bottinelli, L., Gouguenheim, L., Paturel, G., & de Vaucouleurs, G., 1984, *A&AS*, 56, 381
 Cardelli, J.A., Clayton, G.C. & Mathis, J.S., 1989, *ApJ*, 345, 245

- Da Costa, G. S. & Armandroff, T. E., 1990, *AJ*, 100, 162
- Dean, J.F., Warren, P.R. & Cousins, A.W.J., 1978, *MNRAS*, 183, 569
- de Vaucouleurs, G., 1978, *ApJ*, 224, 710
- de Vaucouleurs, G. & Ables, 1965, *PASP*, 77, 272
- Frogel, J.A., Cohen, J.G., & Persson, S.E., 1983, *ApJ*, 275, 773
- Jacoby, G. & Lesser, 1981, *AJ*, 86, 185
- Kells et al., 1998, *PASP*, in preparation
- Landolt, A.U., 1992, *AJ*, 104, 320
- Lee, M. G., Freedman, W. L. & Madore, B. F., 1993, *ApJ*, 417, 553
- Madore, B. F. & Freedman, W. L., 1991, *PASP*, 103, 667
- Madore, B. F. & Freedman, W. L., 1995, *AJ*, 109, 1645
- Madore, B. F. & Freedman, W. L., & Sakai, S., 1997, in *Extragalactic Distance Scale*, ed. M.Livio, M.Donahue, & N.Panagia (Cambridge: Cambridge Univ. Press), 239
- Massey, P. & Armandroff, T.E., 1995, *AJ*, 109, 2470
- Roberts, M.S., 1962, *AJ*, 67, 431
- Sakai, S., Madore, B. F. & Freedman, W. L., 1996, *ApJ*, 461, 713
- Saha, A., Hoessel, J.G., Krist, J. & Danielson, G.E., 1996, *AJ*, 111, 197
- Sandage, A. & Tammann, G., 1974, *ApJ*, 194, 559
- Stanek, K.Z., 1996, *ApJ*, 460, L37
- Stetson, P. B., 1987, *PASP*, 99, 191
- Wilson, C.D., Welch, D.L., Reid, I.N., Saha, A. & Hoessel, J., 1996, *AJ*, 111, 1106
- Yahil, A., Tammann, G.A., & Sandage, A., 1977, *ApJ*, 217, 903
- Yang, H. & Skillman, E.D., 1993, *AJ*, 106, 1448

Figure Captions

Figure 1: An I -band image of IC 10. Three regions used in the analysis are separated by the ellipses drawn.

Figure 2: An $I - (V - I)$ color magnitude diagram for Region 1 (a), Region 2 (b) and Region 3 (c).

Figure 3: Histograms showing I -band luminosity functions for the main body of the galaxy, Region 1 (*top*) and for the halo region (*bottom*).

Figure 4: V and I period-luminosity relations for Cepheid variable stars detected on the COSMIC images.

Figure 5: Multiwavelength fit of a Galactic reddening law to $V I J H K$ apparent distance moduli for IC 10. We obtain a true distance modulus of 24.10 mag. The inset box contains a contour plot showing the χ^2 values from fits to determine the true distance modulus.

Figure 6: Smoothed I -band luminosity functions (*top*), and the edge-detection filter response function (*bottom*). The position of the TRGB is indicated by the highest peak in the response function. The three contour levels represent 1, 2 and 3σ error ellipses.

Figure 7: I -band luminosity functions and the filter response functions for red giant branch stars only.

Figure 8: Color-magnitude diagrams of IC 10 Region 3, shifted by the distance modulus and reddening as indicated on top of each plot.

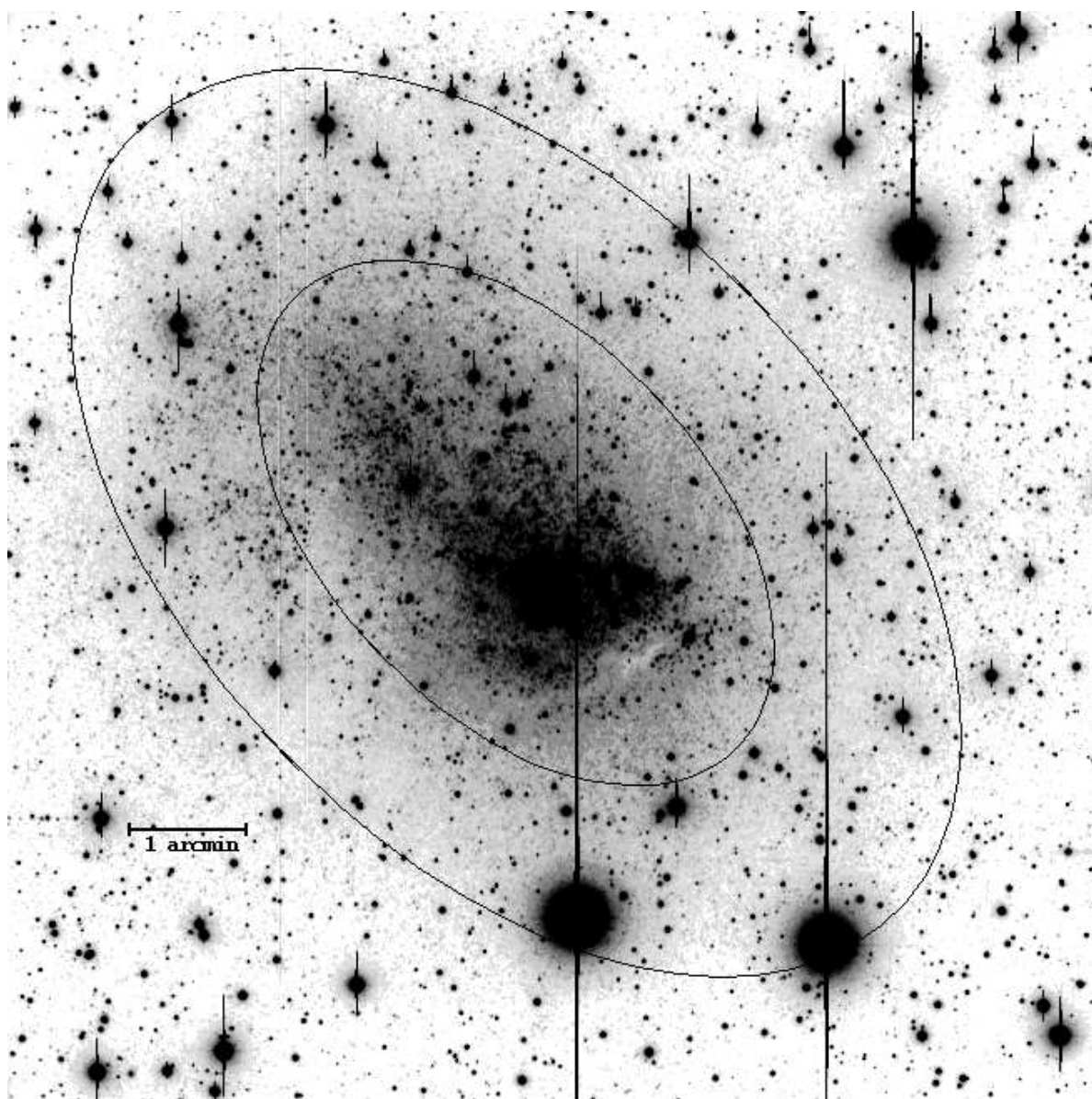
Table 1: *VI* Cepheid data

Cepheid	Period	JD	V	σ_V	I	σ_I
V1	19.12	2450361.7	22.59	0.04	19.91	0.09
V1	19.12	2450362.8	22.45	0.04	19.45	0.10
V2	11.87	2450362.8	23.47	0.06	22.08	0.14
V2	11.87	2450362.8	23.46	0.06	21.43	0.12
V4	57.60	2450361.7	21.65	0.04	19.16	0.09
V4	57.60	2450362.8	21.48	0.05	18.84	0.10
V5	35.29	2450361.7	21.57	0.05	19.24	0.13
V5	35.29	2450362.8	21.52	0.05	18.64	0.10
V6	8.09	2450362.8	25.72	0.54	19.38	0.76
V9	53.36	2450361.7	22.31	0.03	18.56	0.07
V9	53.36	2450362.8	22.05	0.05	18.59	0.10
V11	90.70	2450361.7	21.45	0.03	18.54	0.08
V11	90.70	2450362.8	21.37	0.04	18.06	0.09
V12	48.22	2450361.7	22.23	0.03	19.29	0.08
V12	48.22	2450362.8	22.11	0.04	19.13	0.10

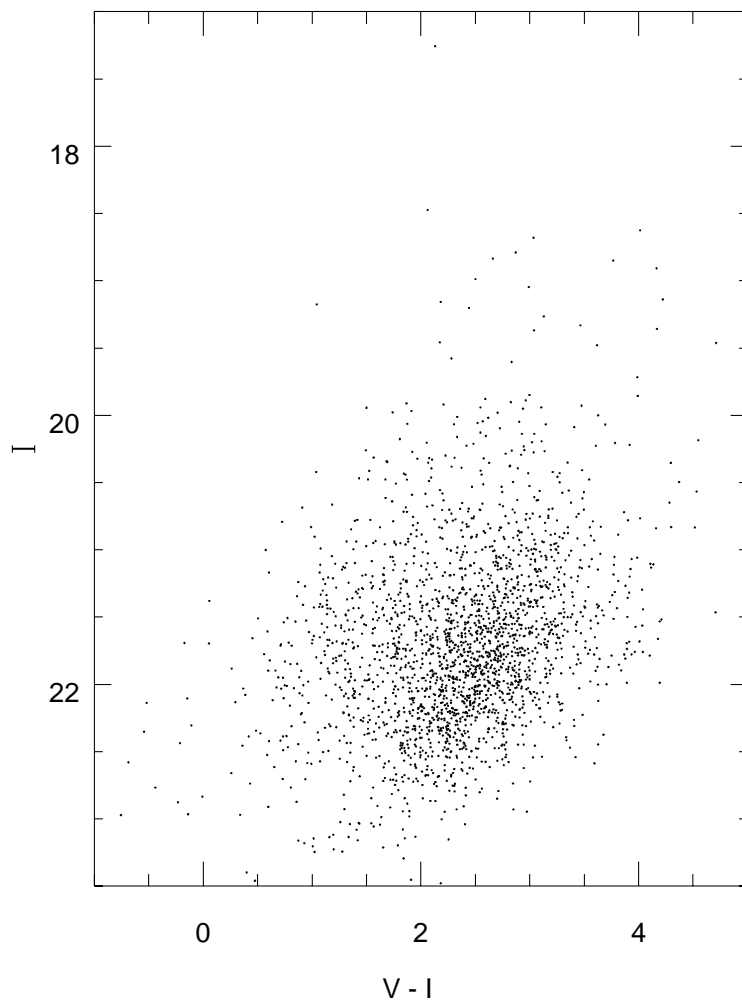
Table 1. **Table 2: Extinction Estimates for IC 10**

Source	$E(B - V)$	A_V	A_I	μ_0	Distance (kpc)
Cepheids(VIJHK) ¹	1.16	3.71	2.19	23.51	504
Wolf-Rayet Stars ²	0.75 – 0.8	2.4 – 2.6	1.4 – 1.5	24.3 – 24.2	724 – 691
Integrated $B - V$ color ³	0.87	2.78	1.64	24.06	649
HII rings ⁴	0.4	1.3	0.8	24.9	955
HII regions ⁵	1.7 – 2.0	5.4 – 6.4	3.2 – 3.8	22.5 – 21.9	316 – 240
Cepheids(JHK) ⁶	0.6 – 1.1	1.6 – 3.5	0.9 – 2.1	24.8 – 23.6	912 – 525
Cepheids(gr) ⁷	0.97	3.10	1.83	23.87	594

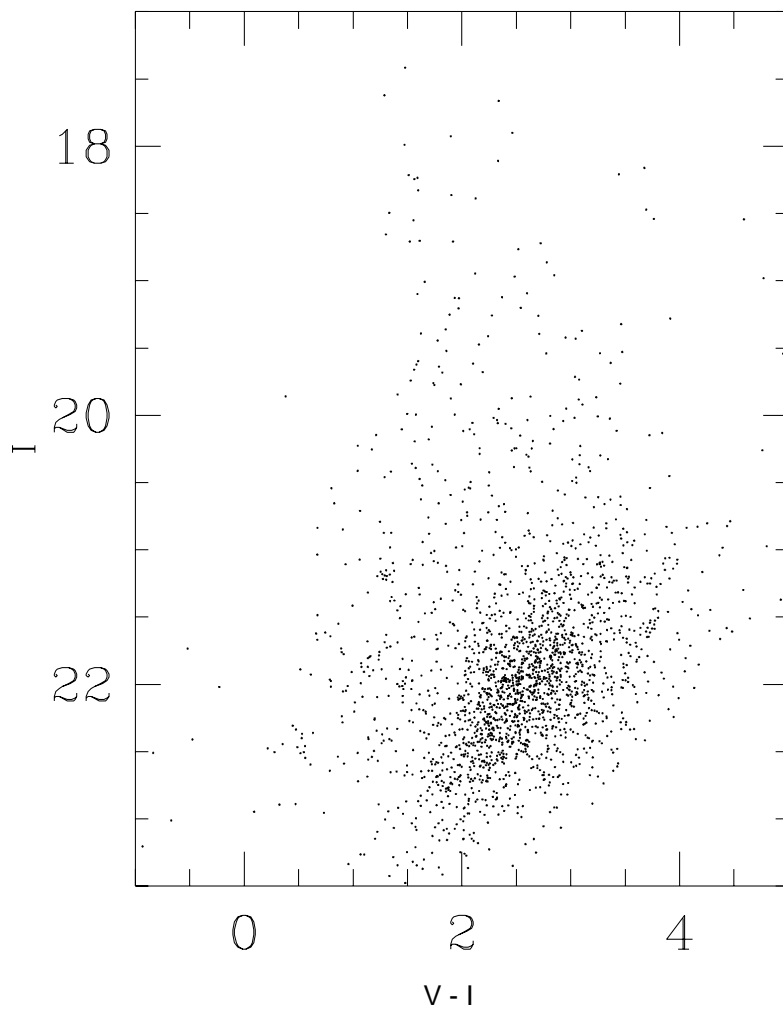
References. — (1) this paper (2) Massey & Armandroff 1995 (3) de Vaucouleurs & Ables 1965 (4) de Vaucouleurs 1978 (5) Yang & Skillman 1993 (6) Wilson et al. 1996 (7) Saha et al. 1996



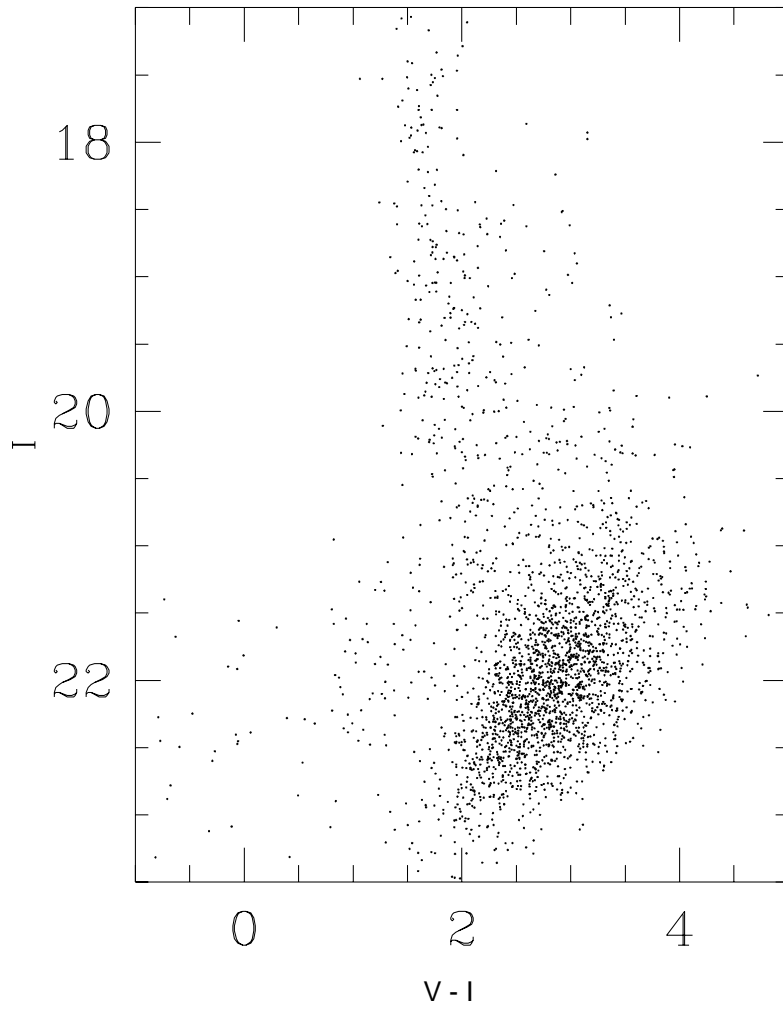
IC 10 Region 1

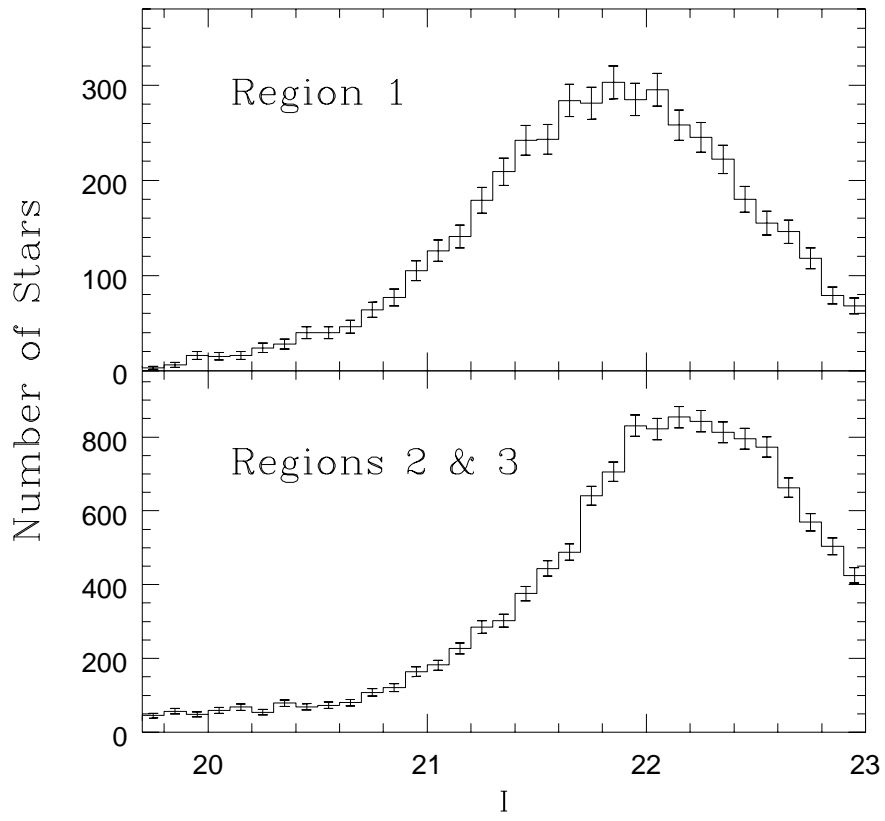


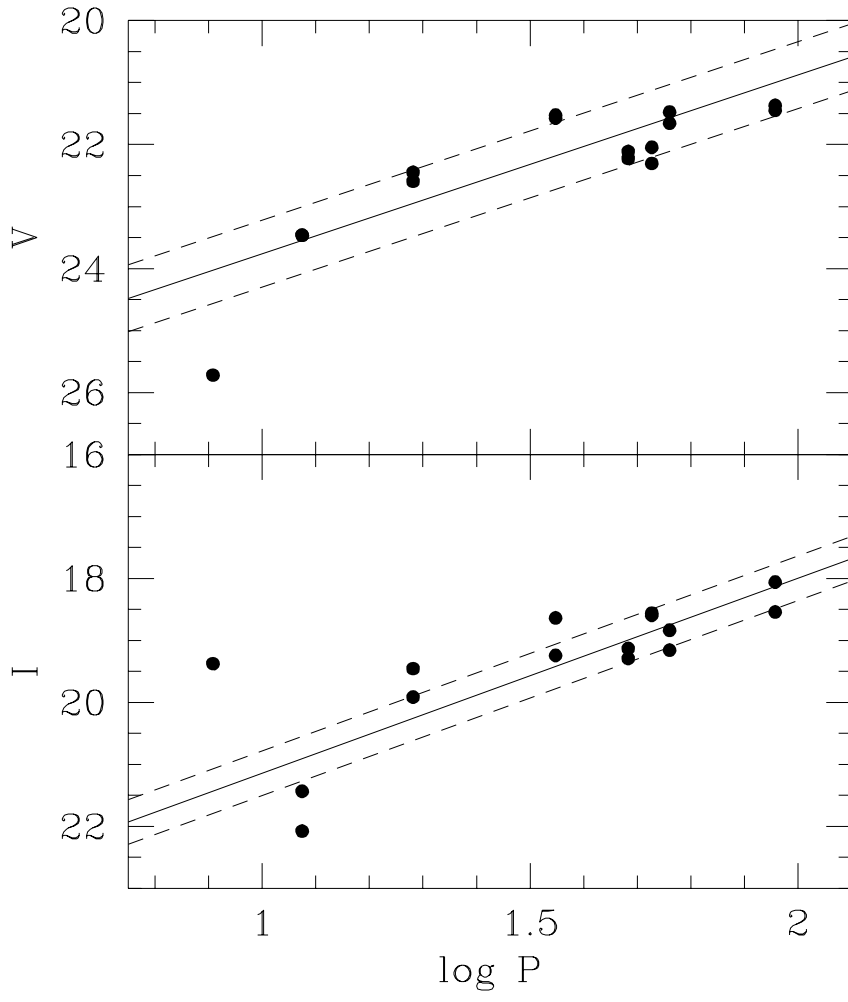
IC 10 Region 2

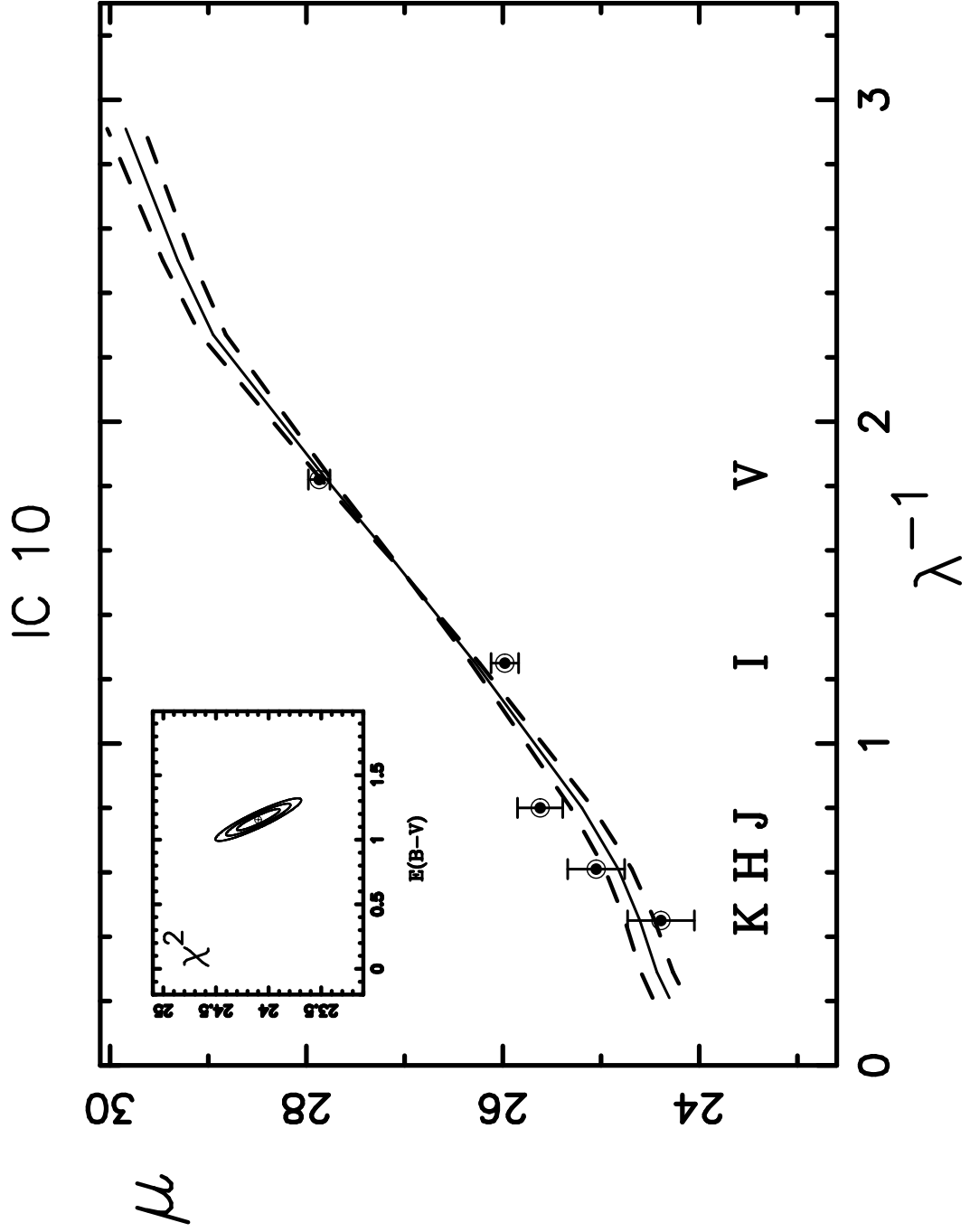


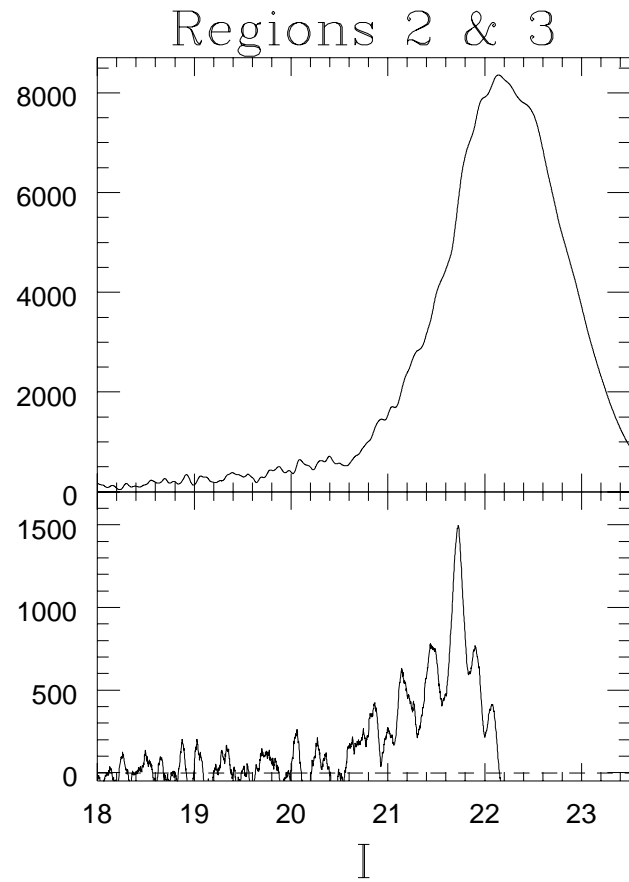
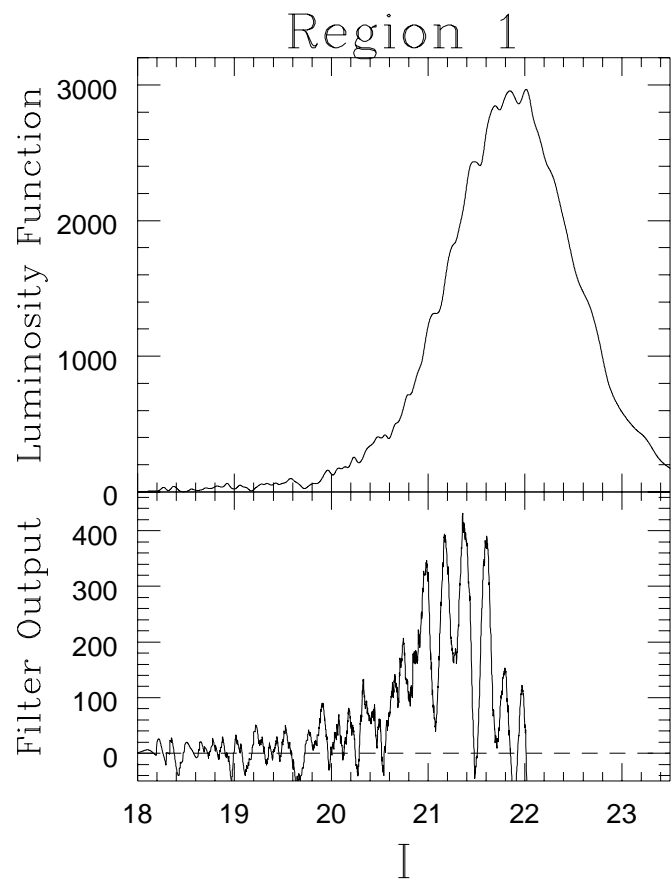
IC 10 Region 3



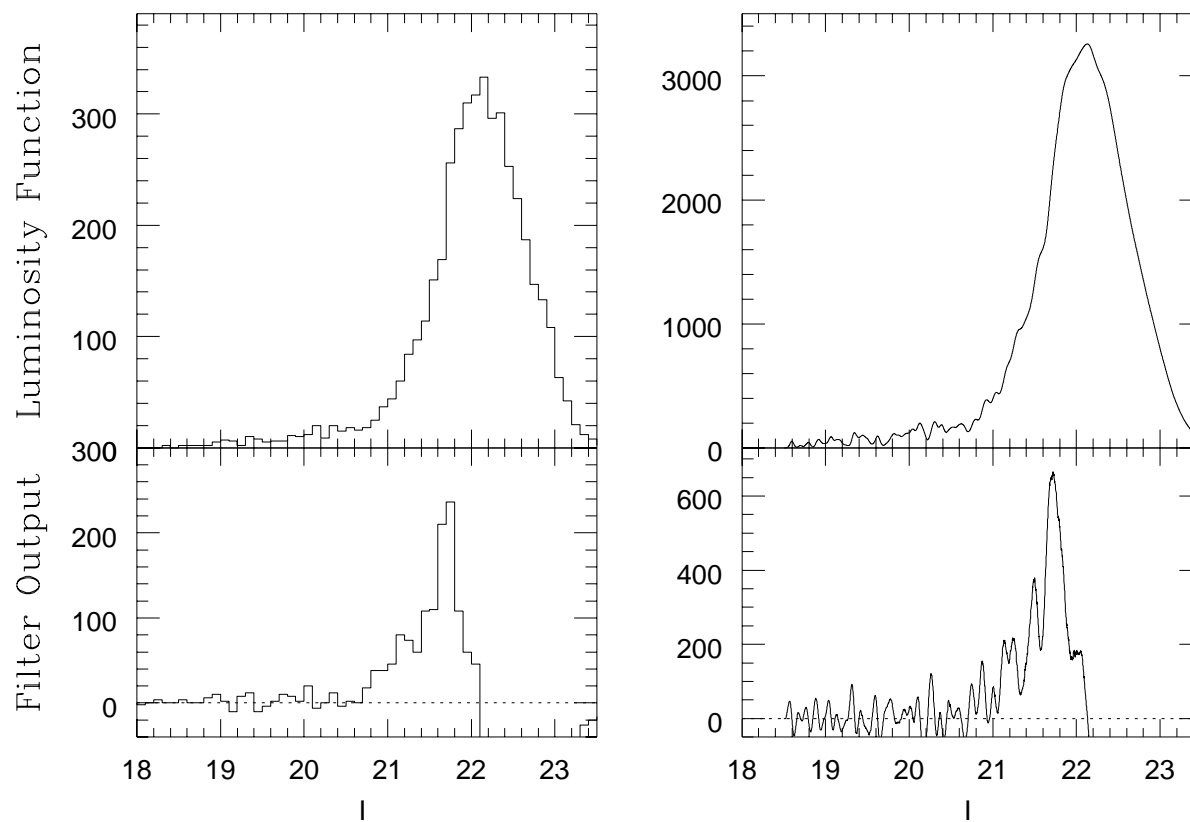


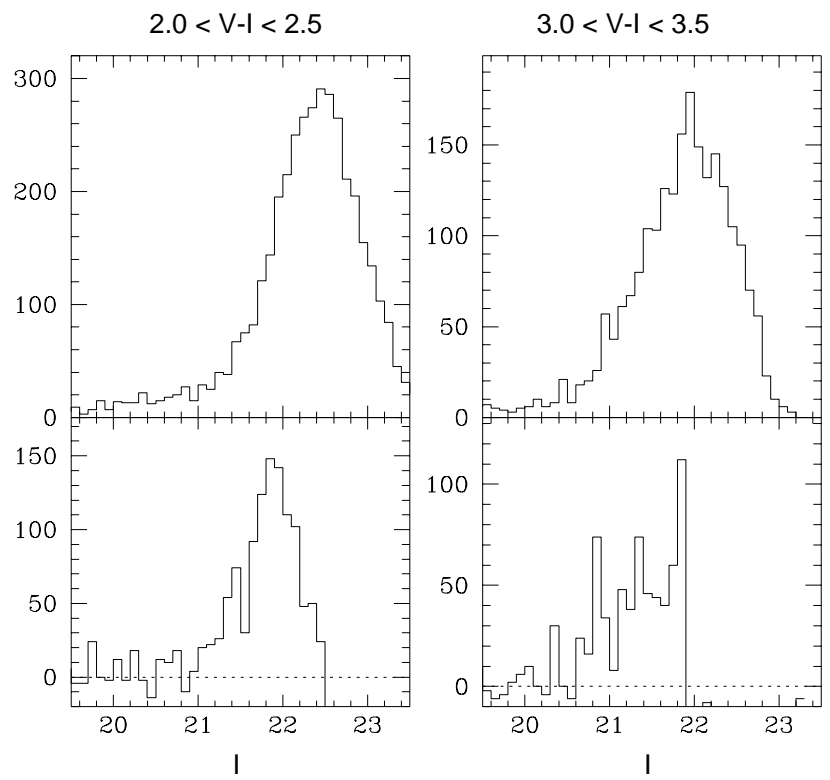






Regions 2 and 3 ($2.5 < V - I < 3.0$)





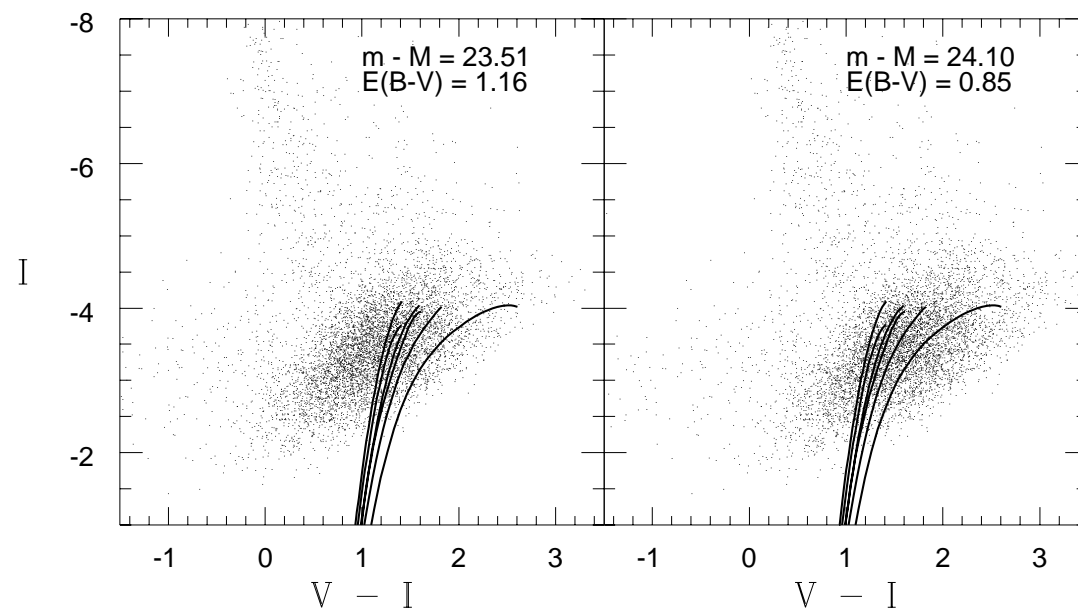


Figure 8